

RESEARCH ARTICLE

Enhancing the control of doubly fed induction generators using artificial neural networks in the presence of real wind profiles

Chaimae Dardabi¹, Abdelouahed Djebli¹, Hamid Choja², Hadoun Aziz³, Abderrahman Mouradi³, Mahmoud A. Mossa^{4*}, Almoataz Y. Abdelaziz⁵, Thamer A. H. Alghamdi^{6,7*}

1 Energetic Laboratory, Department of physics, Faculty of science Tetouan, Abdelmalek Essaadi University, Tetouan, Morocco, **2** Industrial Technologies and Services Laboratory, Higher School of Technology, Sidi Mohamed Ben Abdellah University, Fez, Morocco, **3** Energy, Materials and Computing Physics Research Group, ENS, Abdelmalek Essaadi University, Tetouan, Morocco, **4** Electrical Engineering Department, Faculty of Engineering, Minia University, Minia, Egypt, **5** Faculty of Engineering and Technology, Future University in Egypt, Cairo, Egypt, **6** Wolfson Centre for Magnetism, School of Engineering, Cardiff University, Cardiff, United Kingdom, **7** Electrical Engineering Department, Faculty of Engineering, A-Baha University, Al-Baha, Saudi Arabia

* mahmoud_a_mossa@mu.edu.eg (MAM); AlghamdiT1@cardiff.ac.uk (TAHA)



OPEN ACCESS

Citation: Dardabi C, Djebli A, Choja H, Aziz H, Mouradi A, Mossa MA, et al. (2024) Enhancing the control of doubly fed induction generators using artificial neural networks in the presence of real wind profiles. PLoS ONE 19(4): e0300527. <https://doi.org/10.1371/journal.pone.0300527>

Editor: Wei Yao, Huazhong University of Science and Technology, CHINA

Received: October 13, 2023

Accepted: February 24, 2024

Published: April 17, 2024

Copyright: © 2024 Dardabi et al. This is an open access article distributed under the terms of the [Creative Commons Attribution License](https://creativecommons.org/licenses/by/4.0/), which permits unrestricted use, distribution, and reproduction in any medium, provided the original author and source are credited.

Data Availability Statement: The data are available within the uploaded items.

Funding: The author(s) received no specific funding for this work.

Competing interests: The authors have declared that no competing interests exist.

Abbreviations: β (Degree $^\circ$), Blade pitch angle; λ , Tip Speed Ratio; C_p , Power coefficient; ρ (Kg/m³), Air density; V (m/s), Wind speed; R (m), Blade radius; Ω_g (rad/s), Mechanical speed in the

Abstract

This study tackles the complex task of integrating wind energy systems into the electric grid, facing challenges such as power oscillations and unreliable energy generation due to fluctuating wind speeds. Focused on wind energy conversion systems, particularly those utilizing double-fed induction generators (DFIGs), the research introduces a novel approach to enhance Direct Power Control (DPC) effectiveness. Traditional DPC, while simple, encounters issues like torque ripples and reduced power quality due to a hysteresis controller. In response, the study proposes an innovative DPC method for DFIGs using artificial neural networks (ANNs). Experimental verification shows ANNs effectively addressing issues with the hysteresis controller and switching table. Additionally, the study addresses wind speed variability by employing an artificial neural network to directly control reactive and active power of DFIG, aiming to minimize challenges with varying wind speeds. Results highlight the effectiveness and reliability of the developed intelligent strategy, outperforming traditional methods by reducing current harmonics and improving dynamic response. This research contributes valuable insights into enhancing the performance and reliability of renewable energy systems, advancing solutions for wind energy integration complexities.

1. Introduction

Today, the significance of generating electricity from renewable energy systems is steadily increasing due to the escalating shortage of conventional energy sources and the pressing issue of global warming. Furthermore, the utilization of carbon accounting serves as a crucial technique for estimating the amount of carbon emissions produced by an organization,

generator side; P_t (W), Wind turbine power; p , Number of pole pairs; V_{dc} , DC-link voltage; P_s (W), Q_s (Var), Stator active and reactive powers; ϕ_s, ϕ_r (Wb), Stator and rotor fluxes; V_s, V_r (V), Stator and Rotor voltages; i_s, i_r (A), Stator and rotor currents; ω_s, ω_r (rad/s), Stator and rotor pulsations; ANN, Artificial Neural Network; RSC, Rotor side Converter; GSC, Grid side Converter.

particularly in relation to electricity delivery. This is especially relevant as more industries and individuals actively participate in carbon reduction initiatives [1]. Additionally, the ability to limit the rise in global temperature to 1.5°C and achieve the CO₂ reduction targets by 2050 may rely on the widespread adoption of renewable energy sources (RESs) coupled with increased electrification [2]. In light of advancements in technology, wind energy has emerged as one of the most promising renewable energy sources worldwide, primarily due to its remarkable efficiency and adaptable control capabilities [3].

The conversion of wind energy into mechanical energy within the Wind Energy Conversion System (WECS) necessitates subsequent conversion into electrical energy. This conversion process mandates a harmonious interaction between the mechanical turbine and the electrical generator, emphasizing the need for both an electrical control system for the generator and a mechanical control system for the turbine to ensure reliability and efficiency [4]. However, a critical consideration prior to the development of the controller is the appropriate selection of the generator. Constant-speed operation, despite its drawbacks such as low conversion efficiency, direct impact of varying wind speeds on electrical utility, and high sensitivity to voltage drops and grid faults [5], has been surpassed by the adoption of variable-speed wind generators [6]. Various types of generators are used in wind energy production, including asynchronous, synchronous, DC, and doubly-fed induction generator (DFIG) [7–10]. Presently, the most prevalent generator type employed in wind turbine systems is the doubly-fed induction generator [11–13], which offers an extensive range of advantages [14]. In this system, the rotor windings of the generator are connected to the power grid via an AC-DC-AC converter, while the stator windings are interconnected in series with the grid.

Integration wind energy systems into the power grid can create difficulties due to the unpredictable nature of wind speed. These fluctuations lead to issues such as power oscillations and inconsistencies in energy generation, which can have adverse ripple effects on the electromagnetic torque of the generator. Based on existing literature, researchers express significant concern about enhancing this conversion process. For instance, some focus on increasing the level of wind penetration [15, 16], while others explore the option of utilizing a battery charge controller for energy storage [17–19]. On the other hand, several control approaches have been proposed to enhance the performance of Wind Turbine Systems (WTS) based on Doubly-Fed Induction Generators (DFIG) during normal operations [20]. Among these approaches, two prominent control techniques for DFIG are field-orientation control (FOC) and direct power control (DPC) [21]. Field-orientation control, implemented using a proportional integral (PI) controller, aims to decouple the variables of the machine, making it resemble a direct-current generator [22]. This technique continues to be widely utilized due to its clarity and straightforward implementation [23]. Furthermore, the design of PI parameters significantly influences the dynamic performance of DFIG under FOC. In many applications of Wind Energy Conversion Systems (WECS), the classical PI controller demonstrates satisfactory performance. For instance, in [4], a closed-loop PI controller is employed to adjust the mechanical transfer function's performance parameters, ensuring stability and accuracy. However, the practical effectiveness of this control strategy is limited due to reduced robustness and an inability to adapt to changes in machine parameters caused by factors like grid voltage drops, model inaccuracies, and unexpected variables such as temperature variations. To address these challenges and enhance the robustness of WECS, various advanced control strategies have been proposed as alternatives to FOC, including sliding mode control (SMC) [24] and backstepping control (BSC) [25]. The paper in [24] employs sliding mode control to enhance the performance of variable-speed wind turbine driving a DFIG. While sliding mode control (SMC) has some advantages such as robustness, simplicity, and fast response, it also comes with disadvantages, including the chattering effect and parameter sensitivity, which can

limit the performance and applicability for DFIG control [26, 27]. Consequently, modification and improvements of the SMC technique have been proposed in the literature, such as the super-twisting algorithm [28]. In a different approach the paper in [25] proposes and tests the nonlinear Backstepping control for wind turbine systems. This technique offers benefits such as improved performance, ease of installation, and resilience to external disturbances. However, its drawbacks include complexity and sensitivity. To address these issues, the literature suggests specific improvements and alterations to the backstepping technique, such as adaptive backstepping control [29]. Direct power control (DPC), introduced in 1998 by Neghouchi [30], is another linear control methods widely adopted in various applications, emerging as a competitor to vector control. DPC provides a solution to the challenges posed by sensitivity to parametric variation. Research reveals that DPC significantly enhances dynamic response, allowing for rapid and precise control of generated power [31]. Furthermore, DPC proves effective in minimizing torque and power oscillations within the generator, resulting in a smoother and more stable operational performance [32]. The study demonstrates that the implementation of DPC contributes to improved energy conversion efficiency, optimizing the overall performance of DFIG systems [33]. Additionally, the analysis highlights the simplicity of the control structure employed by dpc, presenting a contrast to traditional vector control methods. This simplicity not only facilitates easier implementation but also contributes to the maintenance of the system [34]. Moreover, the study underscores DPC' notable feature of reduced sensitivity to variations in system parameters, enhancing the robustness and reliability of the DFIG system [31]. However, Direct Power Control (DPC) technique has two main drawbacks: significant power fluctuations and varying commutation frequencies. Various solutions have been proposed to enhance the efficiency and characteristics of Direct Power Control (DPC). One approach involves integrating DPC with various other controllers, including nonlinear controllers and artificial intelligence algorithms. In references [20, 35], authors integrated DPC with sliding mode control (SMC) to overcome the drawbacks of DPC. Reference [20] eliminates the use of hysteresis controllers and switching tables, leading to increased complexity in the implementation process. As a result, adopting the DPC strategy becomes more costly and requires more experimentation. Another proposed solution includes the use of a backstepping controller to enhance the quality of the output current in DFIG system [20–36]. However, the inclusion of a backstepping controller amplifies the complexity and execution challenges associated with Direct Power Control. Additionally, reference [37] presented DPC for a matrix converter feeding a DFIG with a fixed switching frequency. Another novel DPC approach for DFIG, discussed in [38], utilizes L-filter to enhance the quality of DFIG-WTS currents and reduce current, torque, and active power fluctuations. In [39], a combination of fuzzy logic and genetic algorithm is employed to minimize power ripples and enhance the dynamic response of DPC.

In this paper, we address overcome the drawbacks of DPC by employing a combination of Artificial Neural Network (ANN) and the Pulse Width Modulation (PWM) technique for real wind profiles. Artificial Neural Networks (ANNs) serve as intelligent controllers in nonlinear systems, offering several advantages across applications. These include handling large datasets, exhibiting flexibility and nonlinearity, enabling automatic procedures and multitasking, and facilitating rapid processing [40]. The work presented by the author in [41] introduces a novel approach that utilizes an artificial neural network to improve the convergence trajectory and minimize tracking errors in super-twisting sliding mode control. Additionally, in [42], neural networks are applied for stable control of a nonlinear DFIG in wind power systems. The benefits of ANN-based controllers are evident, including reduced peak amplitudes during transient regimes and faster system responses, resulting a shorter time to reach a steady state. Therefore, ANN proves to be a well-established data processing technique, enhancing the understanding and mastery of the control

strategy. The intelligent Direct Power Control (DPC) strategy, incorporating Pulse Width Modulation (PWM), is employed to regulate the Rotor-Side Converter (RSC). This customized DPC strategy significantly differs from the traditional approach by eliminating the conventional switching table and comparators, resulting in a more efficient DPC strategy.

This study entails an experimental investigation of an intelligent Direct Power Control (DPC) strategy, employing an Artificial Neural Network (ANN) controller to enhance current quality and reduce ripples in the Doubly Fed Induction Generator Wind Turbine System (DFIG-WTS). This innovative DPC approach deviates significantly from the conventional method by replacing both the switching table and hysteresis controller, resulting in a more robust DPC strategy.

The main contributions of this paper can be summarized as follows:

- Introduction of an innovative DPC strategy that incorporates artificial neural networks and pulse width modulation (PWM) technique.
- Overcoming the drawbacks and issues associated with DPC.
- Utilization of real-time wind speed data to ensure a reliable basis for analysis.
- Mitigation of ripples in active power and current, leading to an overall enhancement in the performance of the DFIG-WTS.

The paper is structured as follows:

In Section 2, we present a wind energy conversion system model, which is divided into two subsections: wind turbine modeling and double-fed induction generator modeling.

Section 3, formulates the problem by explaining the control configuration of DPC-Classic and outlining the control objectives to be achieved with the intelligent DPC controller.

In Section 4 we describe the implementation of artificial neural network control (ANN) for operating the system, enabling control of active and reactive power.

Section 5 utilizes a real-world profile to analyze experimental results, conducting a comparative study to assess the performance of the two controllers proposed in this work, along with other publications.

Finally, in section 6 we provide a conclusion.

2. Wind energy conversion system modelling

2.1. Wind turbine (HAWT) modelling

The wind turbine plays a crucial role in the wind energy conversion system (WECS) as it transforms kinetic energy into mechanical energy. This component is connected to the generator via a gearbox, which amplifies the rotational speed from the wind turbine to the electric generator [43–51]. To transmit the generator's output to the electrical grid, a control system is utilized [52, 53]. Eq (1) represents the mechanical power P_m generated by the wind turbine [54]:

$$P_m = \frac{1}{2} C_p(\lambda, \beta) \rho \pi R^2 V_{wind}^3 \quad (1)$$

Where ρ is the air density, R is the rotor radius, V_{wind} is the wind speed, and $C_p(\lambda, \beta)$ is the power coefficient, which depends on two aspects: β the blade pitch angle and λ the tip speed ratio, which is defined as:

$$\lambda = \frac{\Omega_{turbine} R}{V_{wind}} \quad (2)$$

$\Omega_{turbine}$ is the angular speed of turbine, related to the mechanical speed of generator Ω_{mec} by the following equation:

$$\Omega_{mec} = G_r \Omega_{turbine} \tag{3}$$

With G_r is the gearbox ratio

Eq (4) depicts the equation of motion that relates the torque and the speed

$$J_{total} \frac{d\Omega_{mec}}{dt} = T_{mec} = T_g - T_{em} - f\Omega_{mec} \tag{4}$$

Where J_{total} is the total mechanical inertia, f is the coefficient of the friction, and T_{mec} T_g T_{em} are successively the mechanical torque, the torque of DFIG, the electromagnetic torque.

In this paper, the model of the power coefficient is defined as [53, 54]:

$$\begin{cases} C_p(\lambda, \beta) = C_1 \left(\frac{C_2}{\lambda_i} - C_3 \cdot \beta - C_4 \right) \cdot e^{\frac{-C_5}{\lambda_i}} + C_6 \lambda \\ \frac{1}{\lambda_i} = \frac{1}{\lambda + 0.08\beta} - \frac{0.035}{\beta^3 + 1} \end{cases} \tag{5}$$

With $C_1 = 0.5176$, $C_2 = 116$, $C_3 = 0.4$, $C_4 = 5$, $C_5 = 21$, $C_6 = 0.0068$ To enable the generator to operate at its optimal speed, it is necessary to ensure that the wind speed is optimal. This can be achieved by utilizing the maximum power point (MPPT), where the power coefficient is kept at its maximum [55].

Fig 1 shows the calculated values of C_p with respect to λ and β . The maximum value of C_p is obtained by fixing λ and β to their optimal values. It is observed in Fig 1 below that $C_p(\lambda, \beta)_{max} = 0.48$ for $\lambda = 8.1$ and $\beta = 0^\circ$.

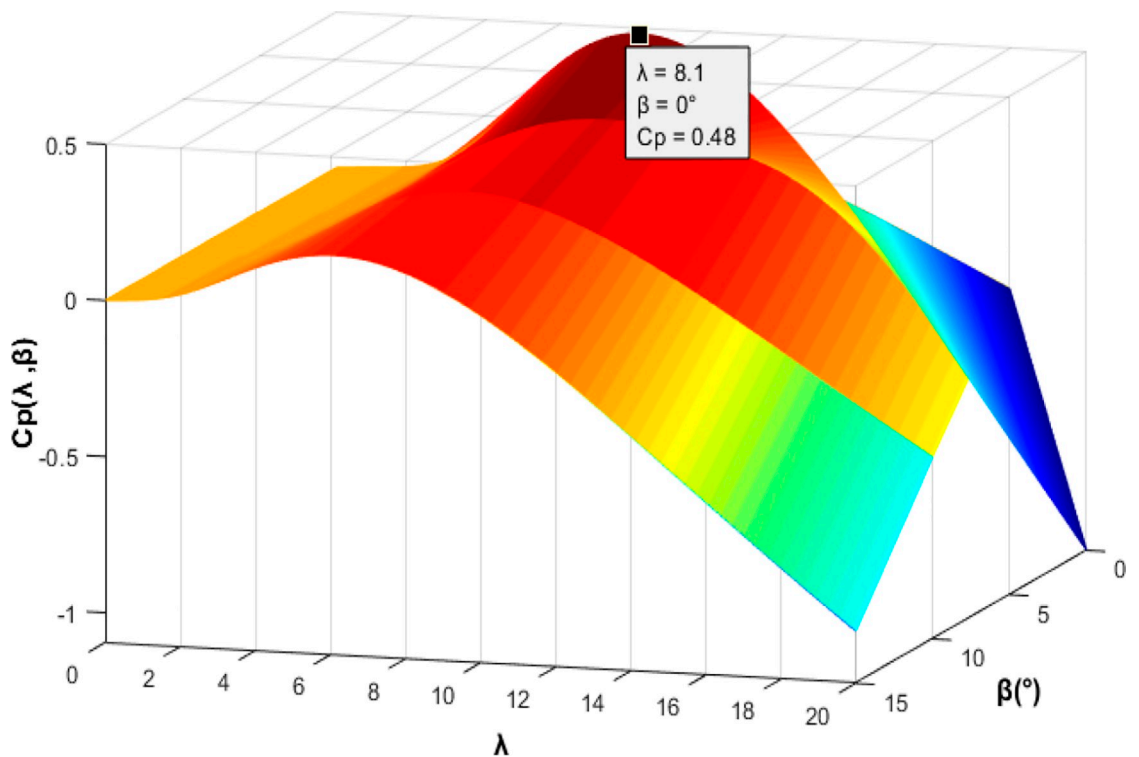


Fig 1. 2D plot of $C_p(\lambda, \beta)$.

<https://doi.org/10.1371/journal.pone.0300527.g001>

2.2. Doubly fed induction generator (DFIG) modelling

The Doubly Fed Induction Generator (DFIG) features two sets of three-phase windings with mutual L_m and self-inductances L_{ss}, L_{rr} [56]. The structure of the DFIG for wind power generation (WPG) is illustrated in Fig 2, where u_s and u_r are the stator and rotor voltages, i_s and i_r are the stator and rotor currents, and U_{dc} is the direct bus voltage.

The voltage equations for the three-phase stator are [52]:

$$E_1 \begin{cases} u_{as} = R_s i_{as} + \frac{d\Phi_{as}}{dt} \\ u_{bs} = R_s i_{bs} + \frac{d\Phi_{bs}}{dt} \\ u_{cs} = R_s i_{cs} + \frac{d\Phi_{cs}}{dt} \end{cases} \quad \text{Where} \quad E_2 \begin{cases} \Phi_{as} = L_{ss} i_{as} + L_m i_{ar} \\ \Phi_{bs} = L_{ss} i_{bs} + L_m i_{br} \\ \Phi_{cs} = L_{ss} i_{cs} + L_m i_{cr} \end{cases} \quad (6)$$

Similarly for the rotor [45]:

$$E_3 \begin{cases} u_{ar} = R_r i_{ar} + \frac{d\Phi_{ar}}{dt} \\ u_{br} = R_r i_{br} + \frac{d\Phi_{br}}{dt} \\ u_{cr} = R_r i_{cr} + \frac{d\Phi_{cr}}{dt} \end{cases} \quad \text{Where} \quad E_4 \begin{cases} \Phi_{ar} = L_{rr} i_{ar} + L_m i_{as} \\ \Phi_{br} = L_{rr} i_{br} + L_m i_{bs} \\ \Phi_{cr} = L_{rr} i_{cr} + L_m i_{cs} \end{cases} \quad (7)$$

During the rotation of the machine, the mutual inductances and the angle between the rotor and stator circuits vary, leading to a dynamic mathematical model [57]. To simplify the mathematical representation, a two-axis model (dq) can be employed, which is less complex than the three-axis model (abc). By utilizing Park’s model, the system can be transformed from a three-phase representation to a direct and quadrature representation.

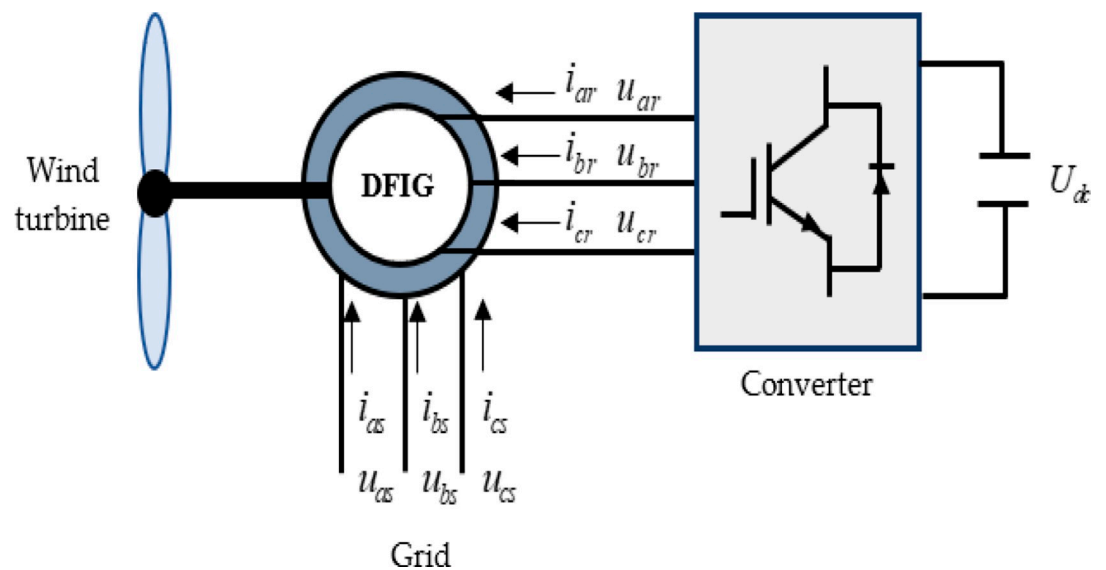


Fig 2. Structure of the DFIG for (WPG).

<https://doi.org/10.1371/journal.pone.0300527.g002>

Utilizing the Park transformation (T_s), the stator voltage equations can be converted to a dq coordinate system in a synchronous reference frame, resulting in the following equations:

$$T_s(E_1) \left\{ \begin{bmatrix} v_{ds} \\ v_{qs} \end{bmatrix} \right\} = T_s \begin{bmatrix} v_{as} \\ v_{bs} \\ v_{cs} \end{bmatrix} = R_s T_s \begin{bmatrix} i_{as} \\ i_{bs} \\ i_{cs} \end{bmatrix} + T_s \frac{d}{dt} \begin{bmatrix} \Phi_{as} \\ \Phi_{bs} \\ \Phi_{cs} \end{bmatrix} \tag{8}$$

$$E_5 \left\{ \begin{array}{l} v_{ds} = R_s i_{ds} + \frac{d}{dt} \Phi_{ds} - \omega_s \Phi_{qs} \\ v_{qs} = R_s i_{qs} + \frac{d}{dt} \Phi_{qs} + \omega_s \Phi_{ds} \end{array} \right. \quad \text{Where} \quad E_6 \left\{ \begin{array}{l} \Phi_{ds} = L_{ss} i_{ds} + L_m i_{dr} \\ \Phi_{qs} = L_{ss} i_{qs} + L_m i_{qr} \end{array} \right. \tag{9}$$

Similarly, the rotor voltage equations given in E_3 can be transformed into the dq frame by Park transformation (T_r), resulting in the new equations of the rotor voltage:

$$T_r(E_3) \left\{ \begin{bmatrix} v_{dr} \\ v_{qr} \end{bmatrix} \right\} = T_r \begin{bmatrix} v_{ar} \\ v_{br} \\ v_{cr} \end{bmatrix} = R_r T_r \begin{bmatrix} i_{ar} \\ i_{br} \\ i_{cr} \end{bmatrix} + T_r \frac{d}{dt} \begin{bmatrix} \Phi_{ar} \\ \Phi_{br} \\ \Phi_{cr} \end{bmatrix} \tag{10}$$

$$E_7 \left\{ \begin{array}{l} v_{dr} = R_r i_{dr} + \frac{d}{dt} \Phi_{dr} - \omega_r \Phi_{qr} \\ v_{qr} = R_r i_{qr} + \frac{d}{dt} \Phi_{qr} + \omega_r \Phi_{dr} \end{array} \right. \quad \text{Where} \quad E_8 \left\{ \begin{array}{l} \Phi_{dr} = L_{rr} i_{dr} + L_m i_{ds} \\ \Phi_{qr} = L_{rr} i_{qr} + L_m i_{qs} \end{array} \right. \tag{11}$$

ω_s and ω_r are the stator and the rotor currents pulsations.

The real and the reactive powers of the DFIG are [58]:

$$E_9 \left\{ \begin{array}{l} P_s = \frac{3}{2} (v_{ds} i_{ds} + v_{qs} i_{qs}) \\ Q_s = \frac{3}{2} (v_{qs} i_{ds} - v_{ds} i_{qs}) \end{array} \right. \tag{12}$$

Eq 13 establishes a relationship between the mechanical and electrical aspects of the machine through the electromagnetic torque [59].

$$T_{em} = \frac{3}{2} p \frac{L_m}{L_{ss}} (\Phi_{qs} i_{dr} - \Phi_{ds} i_{qr}) \tag{13}$$

The vector control by oriented stator field ($\Phi_{ds} = \Phi_s$ and $\Phi_{qs} = 0$) is considered a way to simplify the modeling of the machine because it assures dissociation between its variables and creates a model that resembles a DC machine. This method allows for the decoupling of the stator’s active and reactive powers. Supposing that Φ_{sd} is constant at the permanent regime and R_s is neglected [60], consequently:

$$E_{10} \left\{ \begin{array}{l} v_{ds} = 0 \\ v_{qs} = v_s = \omega_s \Phi_s \end{array} \right. \tag{14}$$

$$E_{11} \left\{ \begin{array}{l} \Phi_s = L_{ss} i_{ds} + L_m i_{dr} \\ 0 = L_{ss} i_{qs} + L_m i_{qr} \end{array} \right. \rightarrow E_{12} \left\{ \begin{array}{l} i_{ds} = \frac{\Phi_s}{L_{ss}} - \frac{L_m}{L_{rr}} i_{dr} \\ i_{qs} = -\frac{L_m}{L_{ss}} i_{qr} \end{array} \right. \tag{15}$$

Replacing E_{12} in E_8 :

$$E_{13} \begin{cases} \Phi_{dr} = \sigma L_{rr} i_{dr} + \frac{L_m}{L_{ss}} \Phi_s \\ \Phi_{qr} = \sigma L_{rr} i_{qr} \end{cases} \rightarrow E_{14} \begin{cases} i_{dr} = \frac{\Phi_{dr}}{\sigma L_{rr}} - \frac{L_m}{\sigma L_{rr} L_{ss}} \Phi_s \\ i_{qr} = \frac{\Phi_{qr}}{\sigma L_{rr}} \end{cases} \quad \text{With } \sigma = 1 - \frac{L_m^2}{L_{ss} L_{rr}} \quad (16)$$

Replacing E_{12} in E_9 and E_{14} in E_{15} :

$$E_{15} \begin{cases} P_s = -\frac{3 L_m}{2 L_{ss}} v_s i_{qr} \\ Q_s = \frac{3}{2} v_s \left(\frac{\Phi_s}{L_{ss}} - \frac{L_m}{L_{ss}} i_{dr} \right) \end{cases} \rightarrow E_{16} \begin{cases} P_s = -\frac{3}{2} \frac{L_m}{\sigma L_{rr} L_{ss}} v_s \Phi_{qr} \\ Q_s = \frac{3}{2} v_s \left(\frac{\Phi_s}{\sigma L_{ss}} - \frac{L_m}{\sigma L_{rr} L_{ss}} \Phi_{dr} \right) \end{cases} \quad (17)$$

The electromagnetic torque and the rotor voltages are:

$$T_{em} = -\frac{3}{2} p \frac{L_m}{L_{ss}} \Phi_s i_{qr} \quad (18)$$

$$E_{17} \begin{cases} v_{dr} = R_r i_{dr} + \sigma L_r \dot{i}_{dr} + e_{qr} \\ v_{qr} = R_r i_{qr} + \sigma L_r \dot{i}_{qr} + e_{dr} + e_\phi \end{cases} \quad \text{with} \quad \begin{cases} e_{qr} = -\omega_r \sigma L_r i_{qr} \\ e_{dr} = \omega_r \sigma L_r i_{dr} \\ e_\phi = \omega_r \frac{L_m}{L_s} \Phi_s \end{cases} \quad (19)$$

3. Problem formulation

3.1 Control configuration

In this paper, the assessment of power performance employs the DPC-Classic strategy instead of repetitive control configurations. DPC offers several advantages, including rapid dynamic response, reduced dependence on machine models, simplified implementation, and low computational complexity [57, 61]. Fig 3 illustrates the conventional DPC approach for controlling wind turbine systems driven by a Doubly Fed Induction Generator (DFIG). Two hysteresis comparators (APHC, RPHC) directly control the DFIG machine’s stator active and reactive powers, while a switching table is utilized for the converter on the rotor side (RSC).

As observed in the preceding figures, the DPC technique necessitates selecting an optimal voltage vector from a switching table to minimize and regulate the discrepancies between the measured and reference powers within predefined hysteresis bands [62].

The hysteresis controller changes its output to “1” if the error of the power (eP_s or eQ_s) reaches a more elevated level [63], also changes its output to “-1” if $eP_s \leq -\Delta P_s$ or $eQ_s \leq -\Delta Q_s$, and to “0” if $-\Delta P_s \leq eP_s \leq \Delta P_s$

Equation E_{16} from the previous section demonstrates that we can determine the relationship of the P_s and Q_s as functions of two rotor flux components in the reference frame (α_r - β_r) that revolve with the DFIG’s rotor. Therefore:

$$\begin{cases} P_s = -\frac{3}{2} \frac{L_m}{\sigma L_{rr} L_{ss}} v_s \Phi_{\beta r} \\ Q_s = \frac{3}{2} v_s \left(\frac{\Phi_s}{\sigma L_{ss}} - \frac{L_m}{\sigma L_{rr} L_{ss}} \Phi_{\alpha r} \right) \end{cases} \quad \text{Where} \quad \begin{cases} \Phi_{\alpha r} = \sigma L_{rr} i_{\alpha r} + \frac{L_m}{L_{ss}} \Phi_s \\ \Phi_{\beta r} = \sigma L_{rr} i_{\beta r} \\ |\Phi_s| = \frac{|\vec{v}_s|}{\omega_s} \end{cases} \quad (20)$$

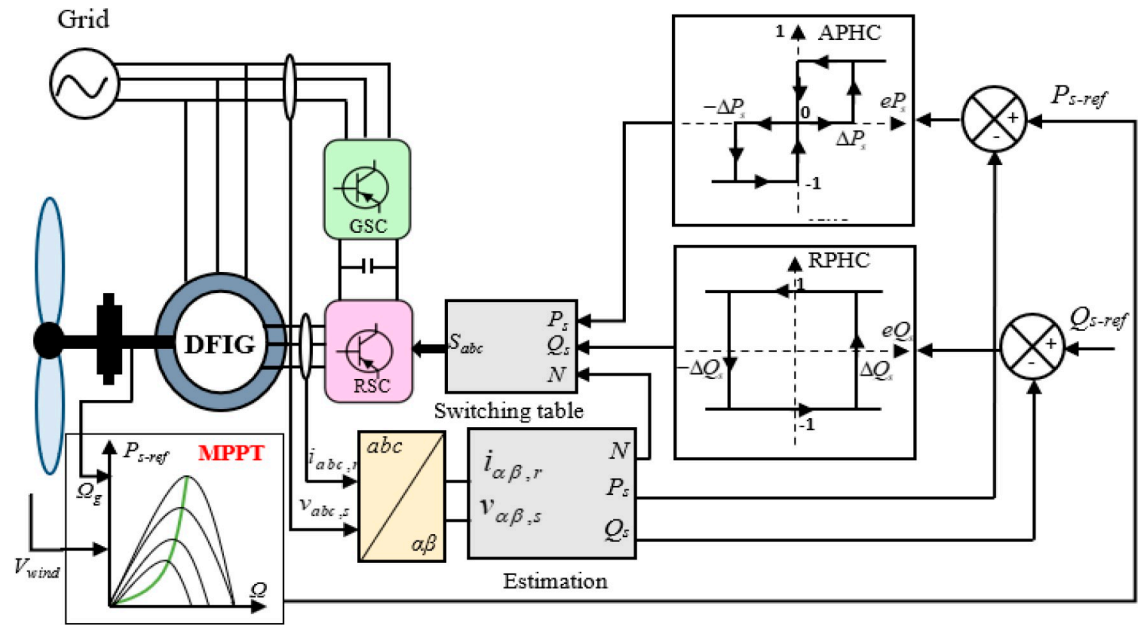


Fig 3. DPC-Classic strategy.

<https://doi.org/10.1371/journal.pone.0300527.g003>

The following expressions show that the active and reactive powers depend directly on the relative angle δ between the stator and rotor flux vectors and their amplitude. Therefore, by modifying δ , it is possible to control P_s and Q_s [57].

$$\begin{cases} P_s = -\frac{3}{2} \frac{L_m}{\sigma L_{rr} L_{ss}} \omega_s |\Phi_s| |\Phi_r| \sin \delta \\ Q_s = \frac{3}{2} \frac{\omega_s |\Phi_s|}{\sigma L_{ss}} \left(\frac{L_m}{L_{rr}} |\Phi_r| \cos \delta - |\Phi_s| \right) \end{cases} \rightarrow \begin{cases} \frac{dP_s}{dt} = -\frac{3}{2} \frac{L_m \omega_s}{\sigma L_{rr} L_{ss}} |\Phi_s| \frac{d(|\Phi_r| \sin \delta)}{dt} \\ \frac{dQ_s}{dt} = \frac{3}{2} \frac{L_m \omega_s}{\sigma L_{rr} L_{ss}} |\Phi_s| \frac{d(|\Phi_r| \cos \delta)}{dt} \end{cases} \quad (21)$$

To select the optimum rotor voltage vector, the relative position of the rotor flux must be determined. Due to the concern with a more stringent control, the evolution space of Φ_r in the reference frame under consideration is divided into six sectors for this purpose [63]. A selection of appropriate vectors applied to the converter on the RSC is shown in Table 1 below. This table enables the rotor flux and powers to be controlled [64, 65].

Table 1. Selection table of optimal vectors (active and reactive power).

		RPHC			-1			
		APHC	1	0	-1	1	0	-1
Sector N concerning the angle δ	1	(330°, 30°)	V ₅	V ₇	V ₃	V ₆	V ₀	V ₂
	2	(30°, 90°)	V ₆	V ₀	V ₄	V ₁	V ₇	V ₃
	3	(90°, 150°)	V ₁	V ₇	V ₅	V ₂	V ₀	V ₄
	4	(150°, 210°)	V ₂	V ₀	V ₆	V ₃	V ₇	V ₅
	5	(210°, 270°)	V ₃	V ₇	V ₁	V ₄	V ₀	V ₆
	6	(270°, 330°)	V ₄	V ₀	V ₂	V ₅	V ₇	V ₁

$V_0 = [0,0,0]$; $V_1 = [1,0,0]$; $V_2 = [1,1,0]$; $V_3 = [0,1,0]$; $V_4 = [0,1,1]$; $V_5 = [0,0,1]$; $V_6 = [1,0,1]$; $V_7 = [1,1,1]$

<https://doi.org/10.1371/journal.pone.0300527.t001>

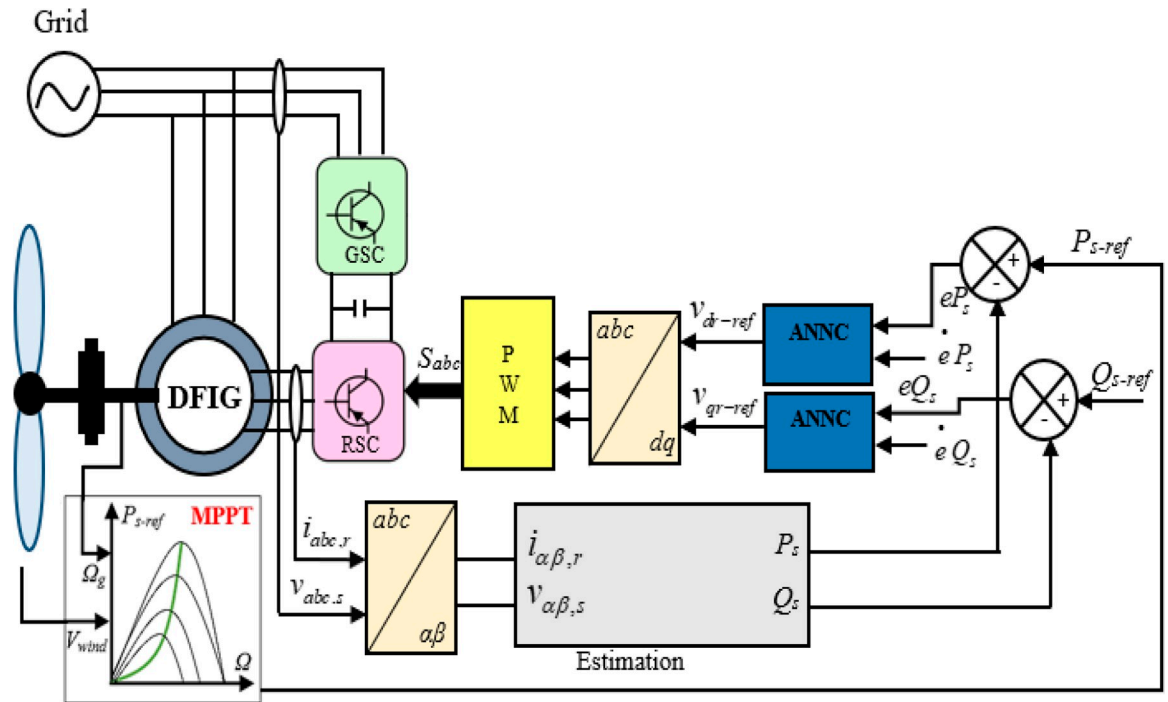


Fig 4. DPC-ANN strategy.

<https://doi.org/10.1371/journal.pone.0300527.g004>

3.2 Control objectives

The direct power control (DPC) strategy has been widely utilized and extensively discussed in DFIG control applications due to its numerous advantages [66, 67]. It effectively decouples active and reactive power, exhibits prompt response without overshoot, and maintains minimal static error, among other benefits. However, the traditional DPC approach suffers from drawbacks such as a high switching frequency, resulting in significant harmonic distortion in

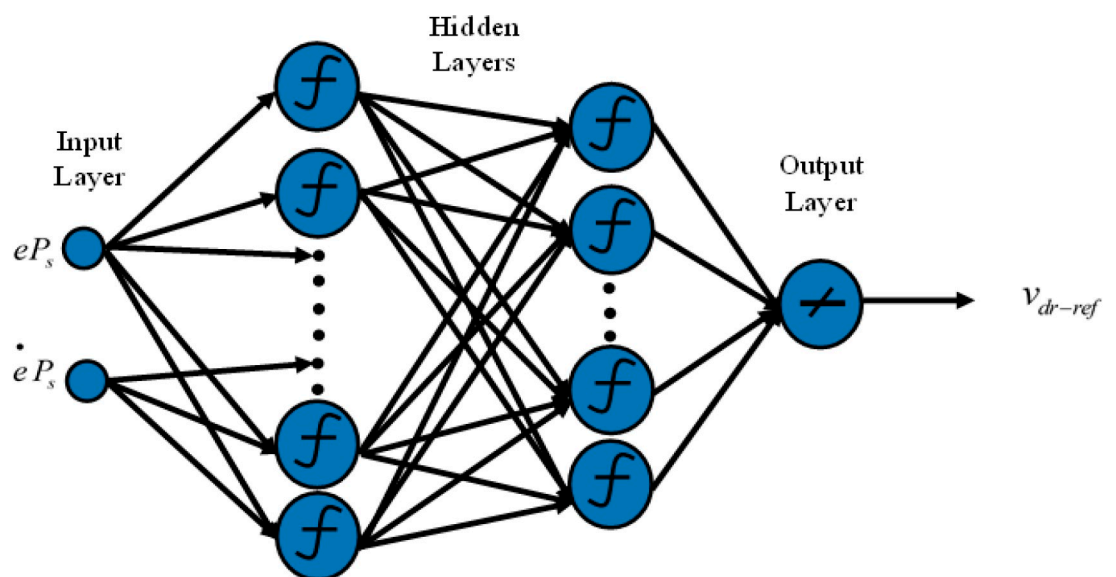
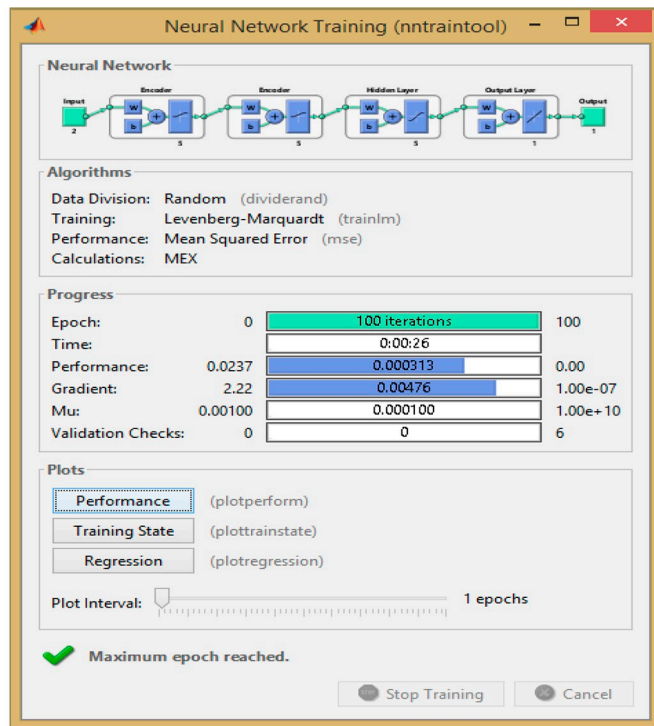


Fig 5. Neural network training (a) and mean squared error (b) for the active power controller.

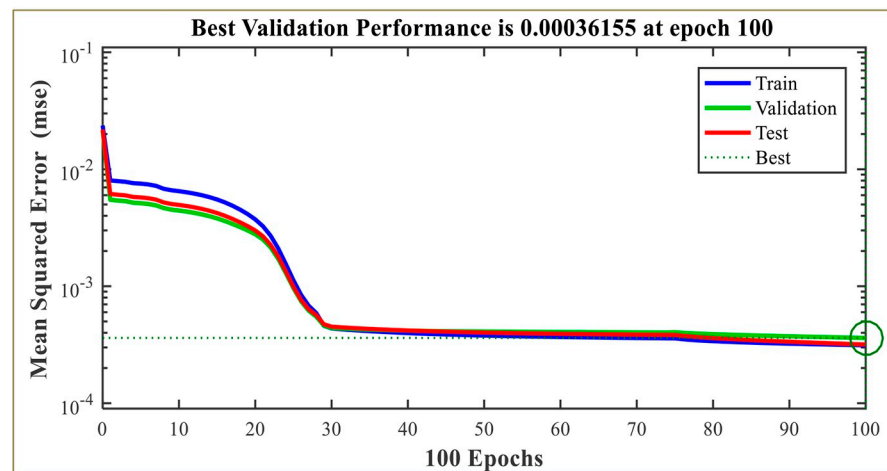
<https://doi.org/10.1371/journal.pone.0300527.g005>

the generated currents and poor current quality, leading to various faults [20, 28–45]. This not only increases maintenance costs but also poses a risk to the grid. Additionally, there are considerable ripples in active and reactive powers due to the variable switching frequency employed in this strategy [68, 69].

To overcome these limitations, this work proposes a novel control method based on Artificial Neural Networks (ANN) [70, 71]. The suggested control approach aims to retain the advantages of the conventional DPC while simultaneously minimizing the THD of current and reducing the ripples in active and reactive powers.



(a)



(b)

Fig 6. Neural network training (a) and mean squared error (b) for the reactive power.

<https://doi.org/10.1371/journal.pone.0300527.g006>

4. System control

Research in neural computing has extensively explored the application of Artificial Neural Networks (ANN) as a data processing technique [53]. This method extends the capabilities of traditional nonlinear automation techniques, providing enhanced effectiveness and reliability in various applications, including identification, control, and filtering. Artificial neurons within ANNs progressively improve their accuracy by learning from input data. Once adequately trained, they can generate results that closely match the desired outcomes [72].

In this research, the classical DPC's hysteresis comparators and switching table are replaced with two neural multilayer perceptron controllers (MLP) and the pulse width modulation technique (PWM). The Levenberg-Marquardt (LM) backpropagation algorithm is employed for the learning process. Fig 4 illustrates the implementation of intelligent DPC using an artificial neural network controller (ANNC) for controlling wind turbine systems with a DFIG. The parameters of the ANN controller presented in this paper can be found in the S1 Appendix. Figs 5 and 6 showcase the learning progress of the active and reactive power controllers. The proposed structure (2-5-5-5-1) for the controllers of active and reactive powers achieves optimal performance quickly, reaching the best results by the 30th and 50th iterations, respectively. Moreover, in Figs 5B and 6B, the Mean Square Error (MSE) progression is depicted concerning the number of iterations for the reactive and active power controllers, respectively. Notably, both controllers achieve a low MSE BY the 100th iteration.

4.1 Artificial neural networks controller for active power

The neural network takes the active power error and its derivatives as inputs, producing the rotor voltage reference as an output. To identify the optimal architecture of the network, the initial MLP controller utilized two hidden layers, as depicted in Fig 7.

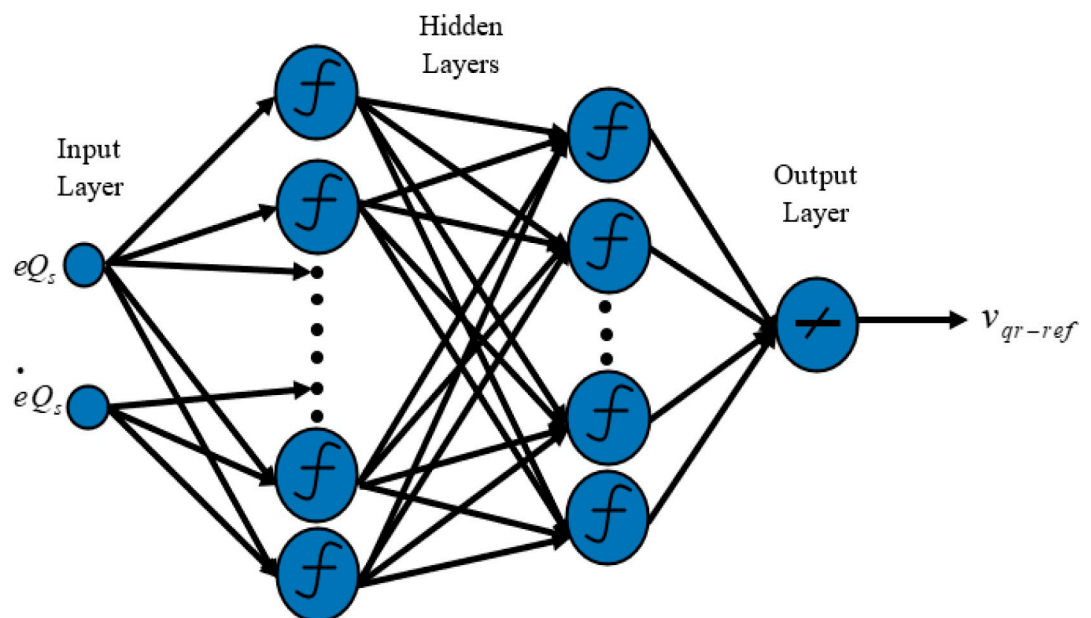
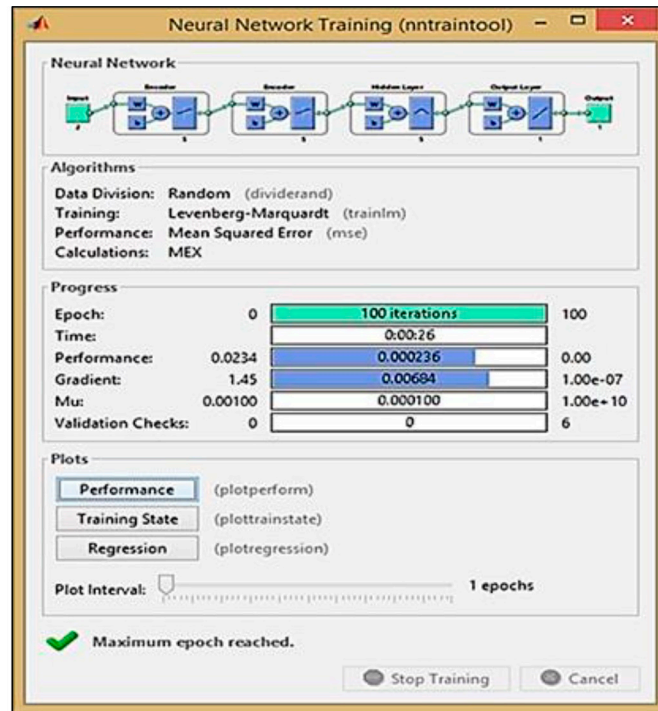
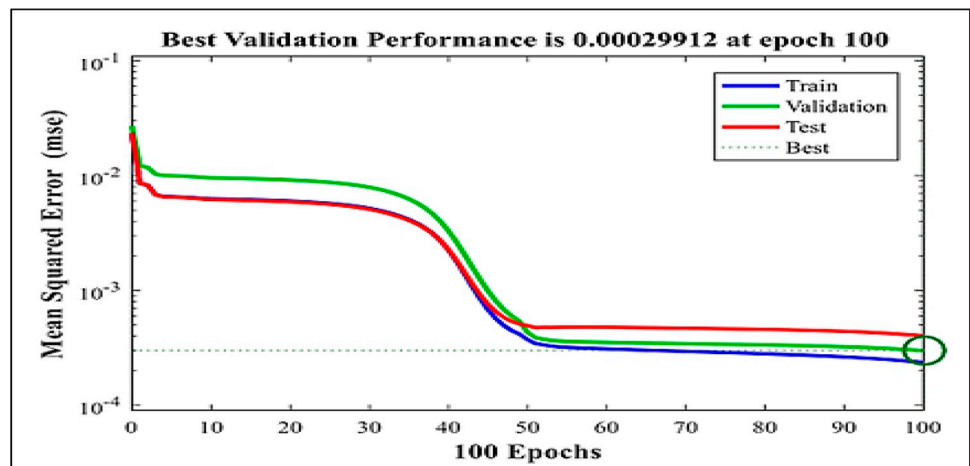


Fig 7. The architecture of the proposed MLP-ANN controller for active power.

<https://doi.org/10.1371/journal.pone.0300527.g007>



(a)



(b)

Fig 8. The architecture of the proposed MLP-ANN controller for reactive power.

<https://doi.org/10.1371/journal.pone.0300527.g008>

4.2 Artificial neural networks controller for reactive power

The neural network takes the reactive power error and its derivatives as inputs, generating the rotor voltage reference as the output. To identify the optimal architecture of the network, the second MLP controller was designed with two hidden layers, as illustrated in Fig 8.

5. Simulation results and discussions

In order to evaluate the dynamic behavior and performance of the proposed novel system, simulations were conducted on a DFIG (1.5KW) using Matlab/Simulink software. The

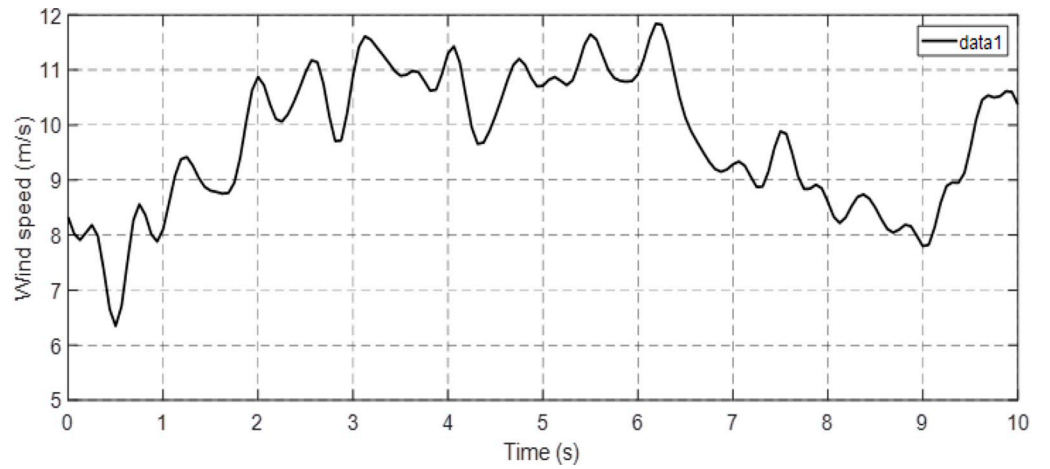


Fig 9. Wind profile of Al-Houceima Morocco city.

<https://doi.org/10.1371/journal.pone.0300527.g009>

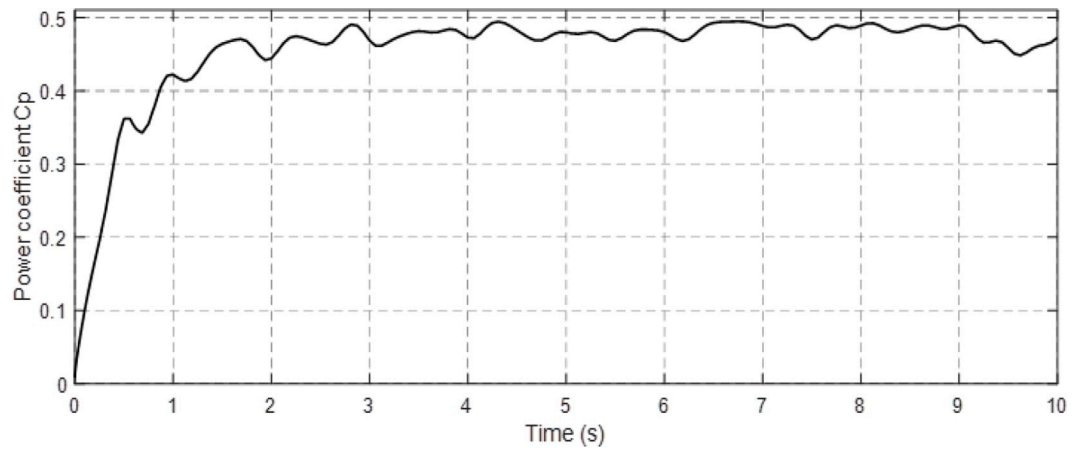


Fig 10. Power coefficient (C_p).

<https://doi.org/10.1371/journal.pone.0300527.g010>

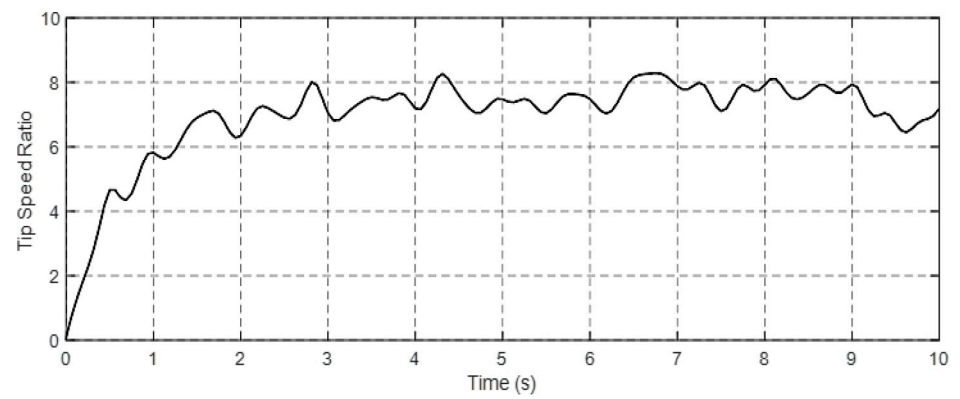


Fig 11. Tip speed ratio (λ).

<https://doi.org/10.1371/journal.pone.0300527.g011>

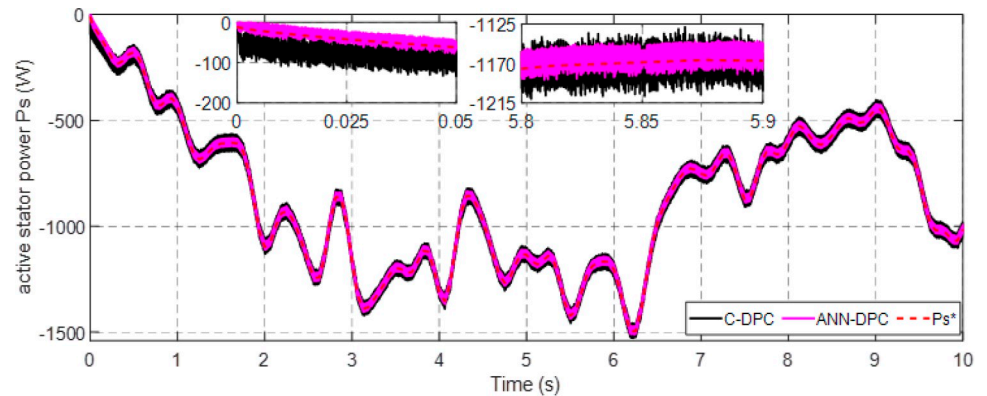


Fig 12. Active power.

<https://doi.org/10.1371/journal.pone.0300527.g012>

parameters of the DFIG utilized in this study can be found in the [S1 Appendix](#). This section focuses on testing and comparing the performance of Classical-DPC and Artificial Neural Network-DPC approaches with reference values. To this end, a wind profile extracted from the Moroccan city of Al-Houceima, as depicted in [Fig 9](#), was employed and the simulation results are presented in the subsequent.

- [Figs 10 and 11](#) depict the correlation between the power coefficient (C_p) and speed ratio (λ) with the wind profile. Changes in wind speed lead to variations in C_p and λ values. The C_p (λ, β) value is approximately 0.5, demonstrating variability, while the maximum tip speed ratio exhibits variability at approximately 8.1.
- [Figs 12 and 13](#) illustrate the convergence of active and reactive power to their reference values, with P_s and Q_s perfectly follow the reference. Even a slight change in wind speed can result in a significant variation in the extracted active power (ranging from 500W to 1500W), with P_s decreasing as wind speed decreases and vice versa. The reactive power reference remains fixed at zero to achieve a unity power factor on the network side.
- [Figs 14 and 15](#) demonstrate the dependence of stator and rotor currents on the applied wind profile, both reaching a maximum value of 5A. It is observed that the value of the rotor/stator currents is linked to both the system and the reference value of P_s .
- [Fig 16](#) presents the rotor current components in the (d, q) frame. The quadrature rotor current varies between approximately 1.2A and 4.7A, influenced by the active power. In

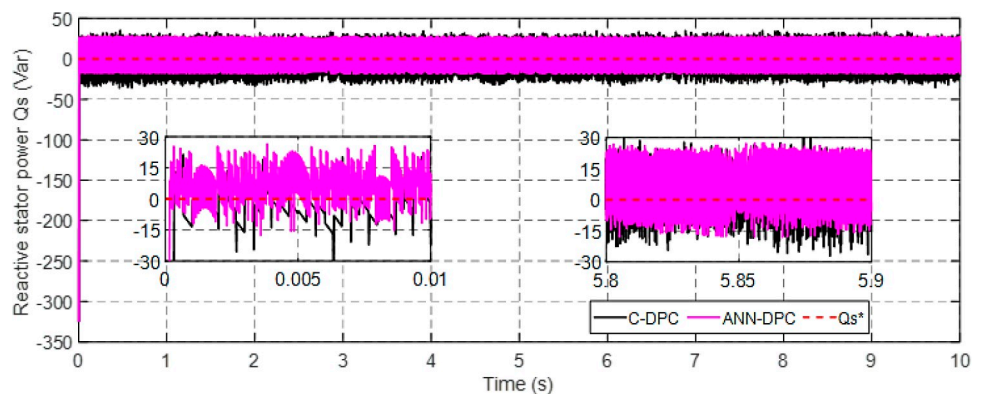


Fig 13. Reactive power.

<https://doi.org/10.1371/journal.pone.0300527.g013>

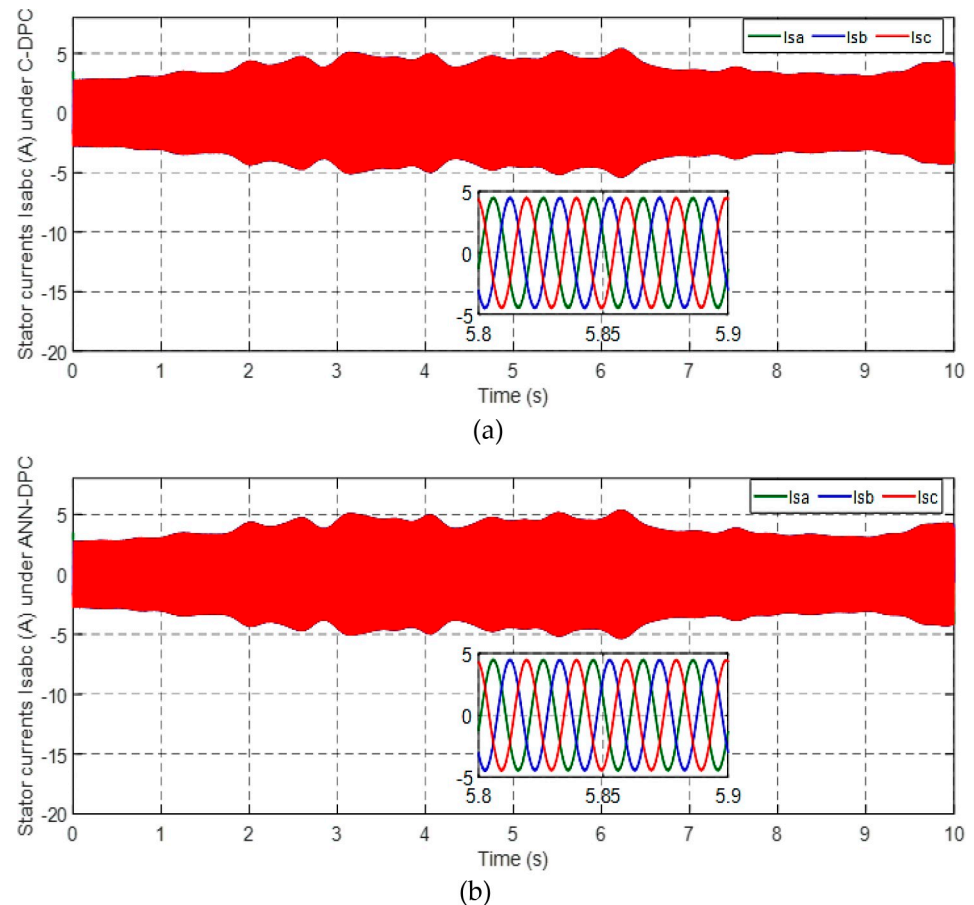


Fig 14. Stator current under C-DPC (a) and ANN-DPC (b).

<https://doi.org/10.1371/journal.pone.0300527.g014>

contrast, the direct rotor current remains stable around 2.4A and is associated with reactive power.

- Fig 17 depicts the power factor of the system, which tends to be close to unity but exhibits slight ripples due to system operation and changes in wind speed.
- Fig 18 displays the analysis of harmonic distortion in the stator current drawn by the DFIG. The Total Harmonic Distortion (THD) resulting from the classical DPC is 1.16%, whereas the THD obtained by the intelligent DPC is 0.81%, signifying a significant reduction compared to that of the classical DPC approach.

6. Conclusion

This research has introduced a robust control method for Double-Fed Induction Generators (DFIG) using an Artificial Neural Network (ANN) in conjunction with an accurate wind profile. The primary objective of this work is to enhance the performance of Direct Power Control (DPC) in DFIG systems. The first section serves as an introduction to the paper. In the second section, the DFIG model is presented, along with the model of the associated wind turbine controlled by the Maximum Power Point Tracking (MPPT) strategy. Furthermore, stator field-oriented techniques are applied to simplify the DFIG model. The third section discusses the classical DPC approach, highlighting its advantages, drawbacks, and desired control

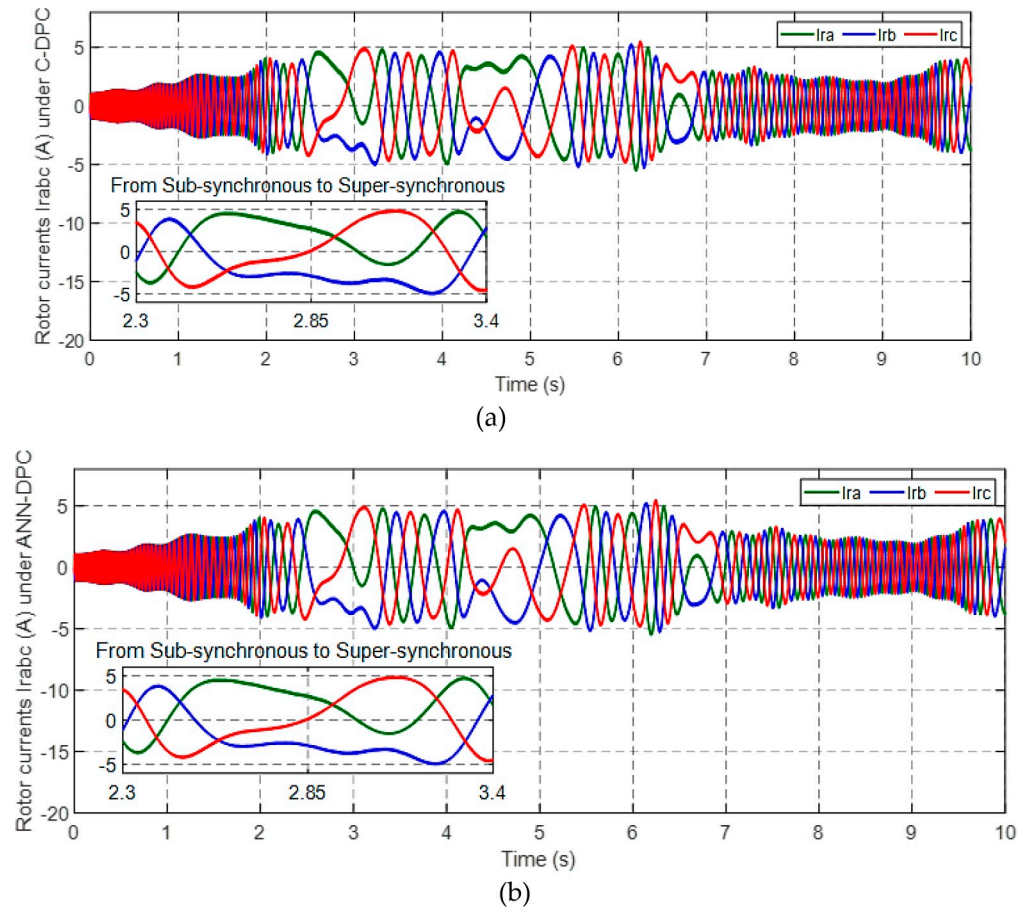


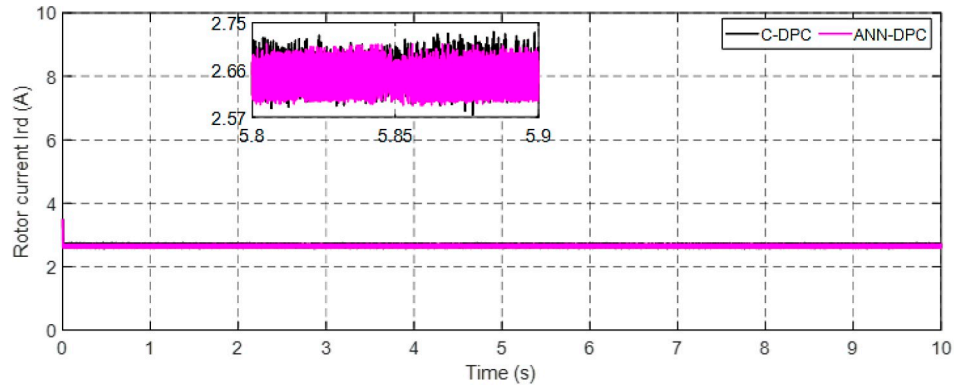
Fig 15. Rotor current under C-DPC (a) and ANN-DPC (b).

<https://doi.org/10.1371/journal.pone.0300527.g015>

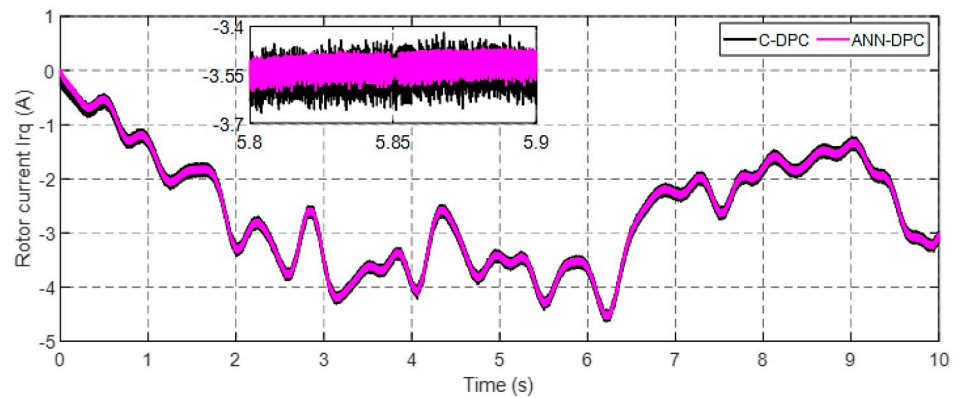
objectives. The fourth section implements an intelligent DPC approach that combines the Pulse Width Modulation (PWM) strategy with a Multilayer Perceptron Artificial Neural Network (MLP-ANN). This intelligent approach enables the control of the stator powers of the DFIG. The fifth section is of utmost importance as it showcases the simulation results of the two controllers using MATLAB/SIMULINK. The main findings of this study can be summarized as follows:

- The DPC maintains its robustness and fast response characteristics.
- The ANN-DPC exhibits superior performance when dealing with varying wind speed profiles.
- The proposed control approach successfully reduces the total harmonic distortion (THD) of the current and mitigates power ripples.
- The efficiency of wind power conversion and the power factor in the system validate the effectiveness of the intelligent DPC technique employed in this study.

One potential direction for future research based on the finding of this paper could involve the investigation and implementation of advanced machine learning algorithms, such as deep learning techniques, to further enhance the control and performance of double-fed induction generators. These advanced algorithms have the potential to learn and adapt to complex wind



(a)



(b)

Fig 16. Direct (a) and quadrature (b) rotor currents.

<https://doi.org/10.1371/journal.pone.0300527.g016>

profiles, optimize control strategies, and improve the overall efficiency and reliability of DFIG systems. Additionally, exploring the integration of advanced optimization techniques, such as genetic algorithms or particle swarm optimization, with the intelligent control approach could offer opportunities for further improvements in the system's performance and stability.

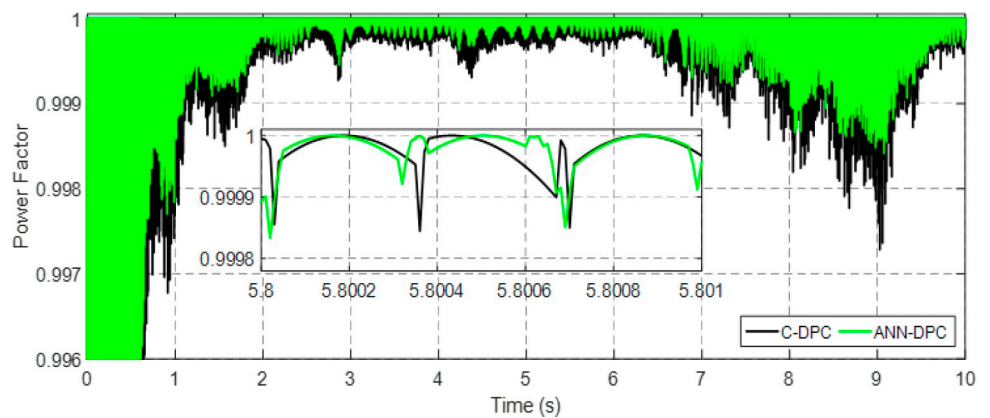
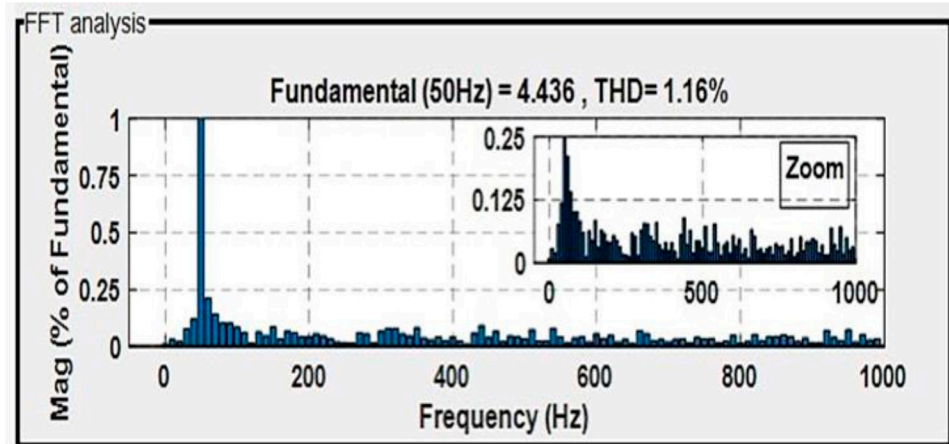
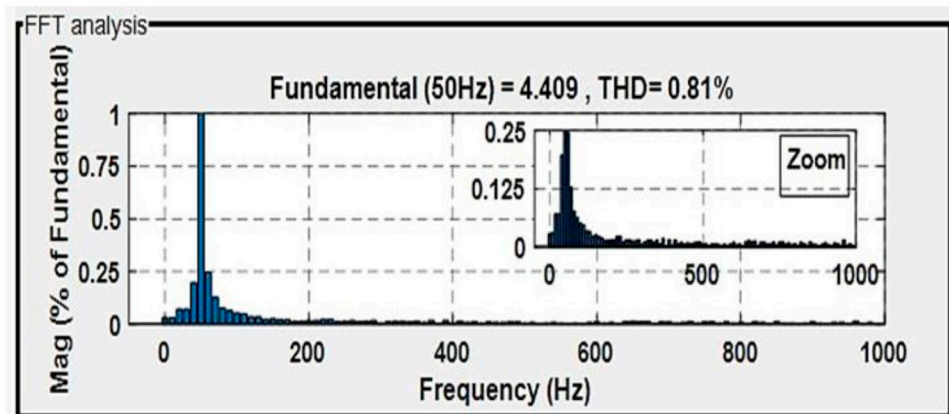


Fig 17. Power factor.

<https://doi.org/10.1371/journal.pone.0300527.g017>



(a)



(b)

Fig 18. The total harmonic distortion of stator current by control: Classical-DPC (a) and ANN-DPC (b).

<https://doi.org/10.1371/journal.pone.0300527.g018>

Supporting information

S1 Data.

(RAR)

S1 Appendix.

(DOCX)

Author Contributions

Conceptualization: Chaimae Dardabi.

Data curation: Abdelouahed Djebli, Almoataz Y. Abdelaziz.

Formal analysis: Hamid Chojaa, Mahmoud A. Mossa, Thamer A. H. Alghamdi.

Funding acquisition: Thamer A. H. Alghamdi.

Investigation: Abdelouahed Djebli, Hadoun Aziz, Almoataz Y. Abdelaziz.

Methodology: Chaimae Dardabi, Abdelouahed Djebli, Mahmoud A. Mossa.

Project administration: Hamid Choja, Mahmoud A. Mossa.

Resources: Chaimae Dardabi, Hadoun Aziz, Abderrahman Mouradi, Thamer A. H. Alghamdi.

Software: Hadoun Aziz, Abderrahman Mouradi, Almoataz Y. Abdelaziz, Thamer A. H. Alghamdi.

Supervision: Hamid Choja.

Validation: Chaimae Dardabi, Abdelouahed Djebli, Hamid Choja.

Visualization: Abderrahman Mouradi, Almoataz Y. Abdelaziz.

Writing – original draft: Chaimae Dardabi, Abderrahman Mouradi, Mahmoud A. Mossa.

Writing – review & editing: Hamid Choja, Mahmoud A. Mossa.

References

1. Chetouani E., Errami Y., Obadi A., Sahnoun S., Choja H. (2022). Optimization Power Control for Rotor Side Converter of a DFIG Using PSO Evolutionary Algorithm. In: Motahir S., Bossoufi B. (eds) Digital Technologies and Applications. ICDTA 2022. Lecture Notes in Networks and Systems, vol 455. Springer, Cham. https://doi.org/10.1007/978-3-031-02447-4_56.
2. IRENA, World energy transitions outlook: 1.5 degrees pathway. 2021. Available from: <https://www.irena.org/Digital-Report/World-Energy-Transitions-Outlook-2022>.
3. Loulilat A., Choja H., El marghichi M., Ettalabi N., Hilali A., Mouradi A., et al. (2023). Enhancement of LVRT Ability of DFIG Wind Turbine by an Improved Protection Scheme with a Modified Advanced Non-linear Control Loop. *Processes* 2023, 11, 1417. <https://doi.org/10.3390/pr11051417>
4. Dardabi C., Akdi M., Djebli A. (2023). Comparative Study of Three Types of Controllers for Variable Speed Wind Turbine. *Lect. Notes Networks Syst.*, vol. 605 LNNS, pp. 783–793, 2023, https://doi.org/10.1007/978-3-031-22375-4_63
5. Mossa M.A., Gam O., Bianchi N. (2022). Dynamic Performance Enhancement of a Renewable Energy System for Grid Connection and Stand-alone Operation with Battery Storage. *Energies*, vol. 15, no. 3, 2022.
6. Meghni B., Choja H., Boulmaiz A. (2020). An optimal torque control based on intelligent tracking range (MPPT-OTC-ANN) for permanent magnet direct drive WECS," *2020 IEEE 2nd Int. Conf. Electron. Control. Optim. Comput. Sci. ICECOCS 2020*, no. December, 2020, <https://doi.org/10.1109/ICECOCS50124.2020.9314304>
7. Mossa M.A., Duc Do T., Saad Al-Sumaiti A., Quynh N. V., Diab A. A. Z. (2021). Effective Model Predictive Voltage Control for a Sensorless Doubly Fed Induction Generator. *IEEE Canadian Journal of Electrical and Computer Engineering*, vol. 44, no. 1, pp. 50–64, winter 2021.
8. Gawande S.P., Porate K.B., Thakre K.L., Bodhe G.L. (2010). Synchronization of Synchronous Generator and Induction Generator for Voltage & Frequency Stability Using STATCOM. In proceedings of the 2010 3rd International Conference on Emerging Trends in Engineering and Technology, Goa, India, 9–21 November 2010; pp. 407–412.
9. Mossa M. A., Saad Al-Sumaiti A., Duc Do T., Zaki Diab A. A. (2019). Cost-Effective Predictive Flux Control for a Sensorless Doubly Fed Induction Generator. *IEEE Access*, vol. 7, pp. 172606–172627, 2019.
10. Mossa M. A., Echeikh H., Iqbal A. (2021). Enhanced control technique for a sensor-less wind driven doubly fed induction generator for energy conversion purpose. *Energy Reports*, vol. 7, pp. 5815–5833, 11, 2021.
11. Mossa M. A., Echeikh H., Zaki Diab A. A., Quynh N. V. (2020). Effective Direct Power Control for a Sensor-Less Doubly Fed Induction Generator with a Losses Minimization Criterion. *Electronics*, vol. 9, no. 8, 2020.
12. Choja H., et al. (2023). Robust Control of DFIG-Based WECS Integrating an Energy Storage System With Intelligent MPPT Under a Real Wind Profile. *IEEE Access*, vol. 11, pp. 90065–90083, 2023, <https://doi.org/10.1109/ACCESS.2023.3306722>
13. Mossa M.A., Abdelhamid M.K., Hassan A.A., Bianchi N. (2022). Improving the Dynamic Performance of a Variable Speed DFIG for Energy Conversion Purposes Using an Effective Control System. *Processes*, vol. 10, no. 3:456, 2022, <https://doi.org/10.3390/pr10030456>

14. Mossa M.A., Mohamed Y. (2012). Novel Scheme for Improving the Performance of a Wind Driven Doubly Fed Induction Generator During Grid Fault. *Wind Eng.* 2012, 36, 305–334, <https://doi.org/10.1260/0309-524X.36.3.305>
15. Ahmadi Kamarposhti M., Geraeli F. (2019). Effect of Wind Penetration and Transmission Line Development in order to Reliability and Economic Cost on the Transmission System Connected to The Wind Power Plants. *Medbiotech J.* 2019; 3(2): 35–40, <https://doi.org/10.22034/mbt.2019.80844>
16. Ahmadi Kamarposhti M., Babak Mozafari S., Soleymani S., Mehdi Hosseini S. (2015). Improving the wind penetration level of the power systems connected to doubly fed induction generator wind farms considering voltage stability constraints". *Journal of Renewable and Sustainable Energy*, 7(4), 2015. <https://doi.org/10.1063/1.4927008>
17. Watil A., El Magri A., Lajouad R., Raihani A., Giri F. (2022). Multi-mode control strategy for a stand-alone wind energy conversion system with battery energy storage. <https://doi.org/10.1016/j.est.2022.104481>.
18. Elaadouli N., Lajouad R., El Magri A., Watil A., Mansouri A., El Myasse I. (2023). An improved control for a stand-alone WEC system involving a Vienna rectifier with battery energy storage management" <https://doi.org/10.1016/j.est.2023.109716>.
19. Chojaa H., Derouich A., Zamzoum O., El Idrissi A. (2024). Robust Control System for DFIG-Based WECS and Energy Storage in real Wind Conditions. *EAI Endorsed Trans Energy Web* [Internet]. 2024 Jan. 16 [cited 2024 Jan. 20]; 11. Available from: <https://publications.eai.eu/index.php/ew/article/view/4856>
20. Wang X., Sun D., Zhu Z. Q. (2017). Resonant-Based Backstepping Direct Power Control Strategy for DFIG Under Both Balanced and Unbalanced Grid Conditions. *IEEE Transactions on Industry Applications*, vol. 53, no. 5, pp. 4821–4830, Sept.–Oct. 2017, <https://doi.org/10.1109/TIA.2017.2700280>
21. Chojaa H., Derouich A., Chehaidia S. E., Zamzoum O., Taoussi M., Elouatouat H. (2021). Integral sliding mode control for DFIG based WECS with MPPT based on artificial neural network under a real wind profile. *Energy Reports*, vol. 7, no. November, pp. 4809–4824, 2021, <https://doi.org/10.1016/j.egy.2021.07.066>
22. Akrama K., Xiao Ming H., Mohamed A. K., Paul B. (2020). Doubly Fed Induction Generator Open Stator Synchronized Control during Unbalanced Grid Voltage Condition. *Energies*, vol. 13, no. 3155, pp. 1–13, 2020.
23. Chojaa H., Derouich A., Taoussi M., Zamzoum O., Hanafi A. (2020). An improved performance variable speed wind turbine driving a doubly fed induction generator using sliding mode strategy. *2020 IEEE 2nd Int. Conf. Electron. Control. Optim. Sci. ICECOCS 2020*, 2020, <https://doi.org/10.1109/ICECOCS50124.2020.9314629>
24. Chojaa H. et al. (2021). Performance improvement of the variable speed wind turbine driving a dfig using nonlinear control strategies. *Int. J. Power Electron. Drive Syst.*, vol. 12, no. 4, pp. 2470–2482, 2021, <https://doi.org/10.11591/ijpeds.v12.i4.pp2470-2482>
25. Boubzizi S., Abid H., El hajaji A., Chaabane M. (2018). Comparative study of three types of controllers for DFIG in wind energy conversion system," *Prot. Control Mod. Power Syst.*, vol. 3, no. 1, pp. 1–12, 2018, <https://doi.org/10.1186/s41601-018-0096-y>
26. Kairous D., Wamkeue R. (2011). Sliding-mode control approach for direct power control of WECS based DFIG. *2011 10th Int. Conf. Environ. Electr. Eng. EEEIC.EU 2011—Conf. Proc.*, pp. 0–3, 2011, <https://doi.org/10.1109/EEEIC.2011.5874836>
27. Mazouz F., Belkacem S., Colak I., Drid S. (2018). Direct Power Control of DFIG by Sliding Mode Control and Space Vector Modulation. *2018 7th International Conference on Systems and Control (ICSC)*, Valencia, Spain, 2018, pp. 462–467, <https://doi.org/10.1109/ICoSC.2018.8587848>
28. Mazouz F., Belkacem S., Boukhalfa G., Colak I. (2021). Backstepping Approach Based on Direct Power Control of a DFIG in WECS. *2021 10th International Conference on Renewable Energy Research and Application (ICRERA)*, Istanbul, Turkey, 2021, pp. 198–202, <https://doi.org/10.1109/ICRERA52334.2021.9598599>
29. Noguchi T., Tomiki H., Kondo S., Takahashi I. (1996). Direct power control of PWM converter without power source voltage sensors. *IAS '96. Conference Record of the 1996 IEEE Industry Applications Conference Thirty-First IAS Annual Meeting*, San Diego, CA, USA, 1996, pp. 941–946 vol.2, <https://doi.org/10.1109/IAS.1996.560196>
30. Kumar B., Sandhu K.S., Sharma R. (2022). Comparative Analysis of Control Schemes for DFIG-Based Wind Energy System. *J. Inst. Eng. India Ser. B* 103, 649–668 (2022). <https://doi.org/10.1007/s40031-021-00660-z>.
31. Zhou P., He Y., Sun D. (2009). Improved direct power control of a DFIG-based wind turbine during network unbalance. *IEEE Trans. Power Electron.*, vol. 24, no. 11, pp. 2465–2474, 2009, <https://doi.org/10.1109/TPEL.2009.2032188>

32. Izanlo A., Gholamian S.A. Kazemi M.V.(2018). Using of four-switch three-phase converter in the structure DPC of DFIG under unbalanced grid voltage condition. *Electr Eng* 100, 1925–1938 (2018). <https://doi.org/10.1007/s00202-017-0671-7>.
33. Savarkar S.V., Singh S.B. (2021). A Comparison of Performance of DPC Technique for DFIG with Using PI and PID Controller. In: Dewan L., Bansal C., R., Kumar Kalla U. (eds) *Advances in Renewable Energy and Sustainable Environment. Lecture Notes in Electrical Engineering*, vol 667. Springer, Singapore. https://doi.org/10.1007/978-981-15-5313-4_12.
34. Xiong L., Li P., Li H., Wang J. (2017). Sliding mode control of DFIG wind turbines with a fast exponential reaching law. *Energies*, vol. 10, no. 11, 2017, <https://doi.org/10.3390/en10111788>
35. Shang L., Hu J.(2012).Sliding-Mode-Based Direct Power Control of Grid-Connected Wind-Turbine-Driven Doubly Fed Induction Generators Under Unbalanced Grid Voltage Conditions. *IEEE Transactions on Energy Conversion*, vol. 27, no. 2, pp. 362–373, June 2012, <https://doi.org/10.1109/TEC.2011.2180389>
36. Yousefi-Talouki A., Zalzar S., Pouresmaeil E. (2019).Direct power control of matrix converter-fed DFIG with fixed switching frequency. *Sustain.*, vol. 11, no. 9, pp. 1–15, 2019, <https://doi.org/10.3390/su11092604>
37. Alhato M.M., Bouallègue S. (2019).Direct power control optimization for doubly fed induction generator based wind turbine systems. *Math. Comput. Appl.* 2019, 24, 77.
38. Pichan M., Rastegar H., Monfared M. (2012).Fuzzy-based direct power control of doubly fed induction generator-based wind energy conversion systems. *2012 2nd International eConference on Computer and Knowledge Engineering (ICCKE)*, Mashhad, Iran, 2012, pp. 66–70, <https://doi.org/10.1109/ICCKE.2012.6395354>
39. Douiria M.R., Essadkib A., Cherkaouic M. (2018).Neural Networks for Stable Control of Nonlinear DFIG in Wind Power Systems. (diouri2018) <https://doi.org/10.1016/j.procs.2018.01.143>.
40. Advantages and Disadvantages of Artificial Neural Networks Posted on February 13, 2023 by Alex Ivankov <https://www.profolus.com/topics/advantages-disadvantages-artificial-neural-networks/>
41. Sami I., Ullah S., Amin S. U., Al-Durra A., Ullah N., Ro J. -S.(2022).Convergence Enhancement of Super-Twisting Sliding Mode Control Using Artificial Neural Network for DFIG-Based Wind Energy Conversion Systems. *IEEE Access*, vol. 10, pp. 97625–97641, 2022, <https://doi.org/10.1109/ACCESS.2022.3205632>
42. Bouiri A., Cherif B., Othmane B, Abdallah A., Chojaa H. (2021).International Journal of Power Electronics and Drive Systems; Yogyakarta Vol. 12, Iss. 4, (Dec 2021): 2443 2450. <https://doi.org/10.11591/ijpeds.v12.i4.pp2443-2450>
43. Huang N., Chen Q., Cai G., Xu D., Zhang L., Zhao W. (2021). Fault Diagnosis of Bearing in Wind Turbine Gearbox Under Actual Operating Conditions Driven by Limited Data With Noise Labels. *IEEE Transactions on Instrumentation and Measurement*, 70, 1–10. <https://doi.org/10.1109/TIM.2020.3025396>
44. Song X., Wang H., Ma X., Yuan X., Wu X. (2023). Robust Model Predictive Current Control for a Nine-Phase Open-End Winding PMSM With High Computational Efficiency. *IEEE Transactions on Power Electronics*, 38(11), 13933–13943. <https://doi.org/10.1109/TPEL.2023.3309308>
45. Liu S., Liu C. (2021). Direct Harmonic Current Control Scheme for Dual Three-Phase PMSM Drive System. *IEEE Transactions on Power Electronics*, 36(10), 11647–11657. <https://doi.org/10.1109/TPEL.2021.3069862>
46. Yang C., Wu Z., Li X., Fars A. (2024). Risk-constrained stochastic scheduling for energy hub: Integrating renewables, demand response, and electric vehicles. *Energy*, 288, 129680. <https://doi.org/10.1016/j.energy.2023.129680>
47. Mo J., Yang H. (2023). Sampled Value Attack Detection for Busbar Differential Protection Based on a Negative Selection Immune System. *Journal of Modern Power Systems and Clean Energy*, 11(2), 421–433. <https://doi.org/10.35833/MPCE.2021.000318>
48. Yang M., Wang Y., Xiao X., Li Y. (2023). A Robust Damping Control for Virtual Synchronous Generators Based on Energy Reshaping. *IEEE Transactions on Energy Conversion*, 38(3), 2146–2159. <https://doi.org/10.1109/TEC.2023.3260244>
49. Duan Y., Zhao Y., Hu J. (2023). An initialization-free distributed algorithm for dynamic economic dispatch problems in microgrid: Modeling, optimization and analysis. *Sustainable Energy, Grids and Networks*, 34, 101004. <https://doi.org/10.1016/j.segan.2023.101004>
50. Zhang X., Gong L., Zhao X., Li R., Yang L., Wang B. (2023). Voltage and frequency stabilization control strategy of virtual synchronous generator based on small signal model. *Energy Reports*, 9, 583–590. <https://doi.org/10.1016/j.egy.2023.03.071>

51. Shao B., Xiao Q., Xiong L., Wang L., Yang Y., Chen Z., Guerrero J. M. (2023). Power coupling analysis and improved decoupling control for the VSC connected to a weak AC grid. *International Journal of Electrical Power & Energy Systems*, 145, 108645. <https://doi.org/10.1016/j.ijepes.2022.108645>
52. Yao L., Wang Y., Xiao X. (2023). Concentrated Solar Power Plant Modeling for Power System Studies. *IEEE Transactions on Power Systems*. <https://doi.org/10.1109/TPWRS.2023.3301996>
53. Mossa M. A., Gam O., Bianchi N., Quynh N. V. (2022). Enhanced Control and Power Management for a Renewable Energy-Based Water Pumping System. *IEEE Access*, vol. 10, pp. 36028–36056, 2022, <https://doi.org/10.1109/ACCESS.2022.3163530>
54. Elouatouat H., Essadki A., Nasser T., Chojaa H. (2022). Integral Sliding Mode Control for DFIG Based Wind Energy Conversion System Using Ant Colony Optimization Algorithm. In: Motahhir S., Bossoufi B. (eds) *Digital Technologies and Applications. ICDTA 2022. Lecture Notes in Networks and Systems*, vol 455. Springer, Cham. https://doi.org/10.1007/978-3-031-02447-4_70.
55. Chojaa H. et al. (2022). Comparative Study of MPPT Controllers for a Wind Energy Conversion System. *Lect. Notes Data Eng. Commun. Technol.*, vol. 110, no. June, pp. 300–310, 2022, https://doi.org/10.1007/978-3-030-94188-8_28
56. Chakib M., Essadki A., Nasser T. (2019). Robust ADRC Control of a Doubly Fed Induction Generator Based Wind Energy Conversion System. In: Hajji B., Tina G.M., Ghoumid K., Rabhi A., Mellit A. (eds) *Proceedings of the 1st International Conference on Electronic Engineering and Renewable Energy. ICEERE 2018. Lecture Notes in Electrical Engineering*, vol 519. Springer, Singapore. https://doi.org/10.1007/978-981-13-1405-6_44.
57. Prasad R. M., Mulla M. A. (2020). Mathematical Modeling and Position-Sensorless Algorithm for Stator-Side Field-Oriented Control of Rotor-Tied DFIG in Rotor Flux Reference Frame. *IEEE Trans. Energy Convers.*, vol. 35, no. 2, pp. 631–639, 2020, <https://doi.org/10.1109/TEC.2019.2956255>
58. Tremblay E., Atayde S., Chandra A. (2011). Comparative study of control strategies for the doubly fed induction generator in wind energy conversion systems: A DSP-based implementation approach. *IEEE Trans. Sustain. Energy*, vol. 2, no. 3, pp. 288–299, 2011, <https://doi.org/10.1109/TSTE.2011.2113381>
59. Zamzoum O., El Mourabit Y., Errouha M., Derouich A., El Ghzizal A. (2018). Power control of variable speed wind turbine based on doubly fed induction generator using indirect field-oriented control with fuzzy logic controllers for performance optimization. *Energy Sci. Eng.*, vol. 6, no. 5, pp. 408–423, 2018, <https://doi.org/10.1002/ese3.215>
60. Djeriri Y. (2020). Lyapunov-based robust power controllers for a doubly fed induction generator. *Iranian Journal of Electrical and Electronic Engineering*, 16(4), 551–558. <https://doi.org/10.22068/IJEEE.16.4.551>
61. Mensou S., Essadki A., Nasser T., Idrissi B. B., Ben Tarla L. (2019). Dspace DS1104 implementation of a robust nonlinear controller applied for DFIG driven by wind turbine. *Renew. Energy*, vol. 147, pp. 1759–1771, 2020, <https://doi.org/10.1016/j.renene.2019.09.042>
62. Mossa M. A., Bolognani S. (2019). Predictive Power Control for a Linearized Doubly Fed Induction Generator Model. *2019 21st International Middle East Power Systems Conference (MEPCON)*, Cairo, Egypt, 2019, pp. 250–257, <https://doi.org/10.1109/MEPCON47431.2019.9008085>
63. Djeriri Y., Meroufel A., Massoum A. (2016). Direct Power Control Based Artificial Neural Network of Doubly Fed Induction Generator for Wind Energy Conversion Systems. *Rev. Roum. Sci. Techn. - Electr. Techn. Energ.*, vol. 54, no. March, pp. 1–22, 2016, <https://doi.org/10.13140/RG.2.1.2245.2886>
64. Djeriri Y., Meroufel A., Belabbes B., Massoum A. (2013). Three-level NPC voltage source converter based direct power control of the doubly fed induction generator at low constant switching frequency. *Rev. des Energies Renouvelables*, vol. 16, pp. 91–103, 2013.
65. Kouadria S., Berkouk E. M., Messlem Y., Denai M. (2018). Improved control strategy of DFIG-based wind turbines using direct torque and direct power control techniques. *J. Renew. Sustain. Energy*, vol. 10, no. 4, 2018, <https://doi.org/10.1063/1.5023739>
66. Yusoff N. A., Razali A. M., Karim K. A., Sutikno T., Jidin A. (2017). A concept of virtual-flux direct power control of three-phase AC-DC converter. *Int. J. Power Electron. Drive Syst.*, vol. 8, no. 4, pp. 1776–1784, 2017, <https://doi.org/10.11591/ijpeds.v8i4.pp1776-1784>
67. Xu L., Cartwright P. (2006). Direct active and reactive power control of DFIG for wind energy generation. *IEEE Trans. Energy Convers.*, vol. 21, no. 3, pp. 750–758, 2006, <https://doi.org/10.1109/TEC.2006.875472>
68. Mensou S., Essadki A., Nasser T., Bououlid Idrissi B. (2020). A direct power control of a DFIG based-WECS during symmetrical voltage dips. *Prot. Control Mod. Power Syst.*, vol. 5, no. 1, 2020, <https://doi.org/10.1186/s41601-019-0148-y>

69. Djeriri Y. et al.(2012).Using Space Vector Modulation Technique to Improve Direct Power Control Strategy of Doubly Fed Induction Generator Based Wind Energy Conversion Systems. no. October, pp. 481–487, 2012.
70. Gao S., Zhao H., Gui Y., Zhou D., Terzija V., Blaabjerg F.(2021).A Novel Direct Power Control for DFIG with Parallel Compensator under Unbalanced Grid Condition. *IEEE Trans. Ind. Electron.*, vol. 68, no. 10, pp. 9607–9618, 2021, <https://doi.org/10.1109/TIE.2020.3022495>
71. Cinar A. C.(2020).Training Feed-Forward Multi-Layer Perceptron Artificial Neural Networks with a Tree-Seed Algorithm Training Feed-Forward Multi-Layer Perceptron Artificial Neural Networks with a Tree-Seed Algorithm. *Arab. J. Sci. Eng.*, no. September, 2020, <https://doi.org/10.1007/s13369-020-04872-1>
72. Aroussi H. A., Ziani E. M., Bouderbala M., Bossoufi B.(2020).Enhancement of the direct power control applied to DFIG-WECS. *Int. J. Electr. Comput. Eng.*, vol. 10, no. 1, pp. 35–46, 2020, <https://doi.org/10.11591/ijece.v10i1.pp35-46>